



12<sup>th</sup> IEA Heat Pump Conference 2017



# Non-intrusive characterization of thermally driven heat pumps

Oliver Buchin <sup>a,\*</sup>, David Dehler <sup>b</sup>, Christian Koglin <sup>c</sup>,  
Paul Schmitt-Gehrke <sup>a</sup>, Felix Ziegler <sup>a</sup>

<sup>a</sup> Technische Universität Berlin, KT2, Marchstraße 18, 15587 Berlin, Germany

<sup>b</sup> Adakom GmbH, Bühringstr. 8, 13086 Berlin, Germany

<sup>c</sup> Physikalisch Technische Bundesanstalt, Fachbereich 7.5, Abbestr. 2-12, 10587 Berlin, Germany

---

## Abstract

The operational behavior of thermally driven heat pumps is characterized by flow and temperature measurements at the main heat exchangers. Non-intrusive ultrasonic clamp-on flow measurements and clamp-on temperature measurement are often the only option in field-installations with respect to process interruption or cost. However, the accuracy of these non-intrusive methods is sensitive to flow profile and piping geometry rendering them usually less accurate than intrusive methods.

A physical model is applied to allocate the effective measurement uncertainty according to the influences of temperature, flow velocity, piping geometry, fluid properties, and flow profile. The sensitivities of the important parameters and their impact on the deduced uncertainties in nominal and part-load operation are analyzed. As an example, data of an absorption heat pump designed at Technische Universität Berlin are analysed.

Results show that the relative uncertainty of heat flow measurement is highest in part load operation and has a large impact on the uncertainty of seasonal performance indicators. Acceptable uncertainties can be achieved by applying an expert system that optimizes the measurement configuration and corrects the influence of flow disturbances with a physical modelling approach.

© 2017 Stichting HPC 2017.

Selection and/or peer-review under responsibility of the organizers of the 12th IEA Heat Pump Conference 2017.

Keywords: Sorption heat pump, Ultrasonic flow measurement, heat metering, clamp-on measurement, COP

---

## 1. Introduction

Monitoring of heating and cooling systems is a basis for the identification of potentials to increase their energy efficiency. For instance, in the monitoring study of Kühn et al. [1] field installations of gas driven absorption heat pumps have shown a significantly lower efficiency than expected. The lower efficiency was attributed to a deficient system layout, inappropriate control parameters, and installation faults. The studies of Miara et al. [2,3] have shown that systems with electrical heat pumps quite often have a lower efficiency in the field than expected under laboratory conditions. Inadequate loading strategies of the storage tank, oversized pumps, bypass flows in three-way-valves, and mistimed operation of the charge pump were detected as typical deficits in these systems. Given these findings, it has to be assumed that there remains a large optimization potential for thermally driven heat pumps in field installations. Thus, measurements for monitoring under such field conditions are essential for system optimization. They have to be both simple to install and accurate because to separate the performance of the heat pump from the hydraulic periphery it is of importance to measure with high accuracy. All of the studies cited above used inline techniques for measurement to determine the relevant heat flows, which is however not always the most practical way of measuring.

---

\* Corresponding author. Tel.: +49-30-314 73720; fax: +49-30-314 22253.

E-mail address: oliver.buchin@tu-berlin.de.

Heat flows can be measured non-intrusively with ultrasonic clamp-on flow meters and clamp-on thermometers. Ultrasonic clamp-on meters show various advantages over intrusive measurement techniques such as avoidance of pressure losses, installation during operation without pipe works, or independency of electrical conductivity of the flowing media. However, non-intrusive methods are not a state-of-the-art method for heat pump characterization as uncertainties remain higher than for inline methods, such as electromagnetic, inertial, or ultrasonic flow meters. Inline meters obtain higher accuracy as the flow can be conditioned, the flow path geometry can be determined with high accuracy, and the flow meter can be calibrated before installation.

This paper analyses the uncertainty of the performance under nominal and part load conditions for measurements with non-intrusive techniques, allowing the applicability under field conditions to be evaluated. A rigorous uncertainty balance is applied according to JCGM 100:2008 [4]. Two types of experimental conditions are analyzed; first, laboratory conditions with high measurement accuracy and second, field conditions with lower accuracy.

## 2. Methods

### 2.1 Performance indicators of thermally driven heat pumps

The Coefficient of Performance (COP) represents the capacity  $\dot{Q}_1$  of a thermally driven heat pump in relation to the supplied power (driving heat  $\dot{Q}_2$  and auxiliary electrical power) to the unit [5]. All coefficients only apply under stationary operating conditions. Neglecting the auxiliary energy input, the thermal COP of a heat pump is defined as follows:

$$COP = \frac{\dot{Q}_1}{\dot{Q}_2}. \quad (1)$$

The Energy Efficiency Ratio (EER) is a value derived from energy measurements of a time interval  $dt$  and such it is an integral performance indicator:

$$EER = \frac{\int \dot{Q}_1 dt}{\int \dot{Q}_2 dt}.$$

Seasonal performance is indicated with a seasonal EER (SEER) respectively. These are the weighted mean of the part load energy efficiencies under rated conditions:

$$SEER = \sum_i w_i EER_i. \quad (2)$$

The same performance figures can also be applied for thermally driven chillers with the cooling capacity  $\dot{Q}_0$  used in the numerator instead of the heating capacity.

### 2.2 Ultrasonic clamp-on flow measurement

Ultrasonic flow meters typically measure the transit time difference of two modulated ultrasonic signals, one passing with and the other against the flow direction. The volumetric flow rate  $\dot{V}$  is related to the transit time difference  $\Delta t$  and the cross sectional pipe area  $A$  as follows [6]:

$$\dot{V} = Av = A C_{Profile} C_{Trans} \frac{\Delta t}{2t}. \quad (3)$$

The mean flow velocity  $v$  is determined by the transit time difference  $\Delta t$ , the absolute transit time  $t$ , and two coefficients,  $C_{Trans}$  and  $C_{Profile}$ . The acoustic calibration coefficient  $C_{Trans}$  accounts for the influences of the geometry and the acoustic properties of the ultrasonic transducers. The flow profile coefficient  $C_{Profile}$  relates the area-averaged velocity to the path-averaged velocity, which is physically measured from the transit time difference of the ultrasonic signal.  $C_{Profile}$  is dependent on the flow profile, thus on Reynolds number. The empiric relations of flow profile with Reynolds-number usually assume axially symmetric profiles.

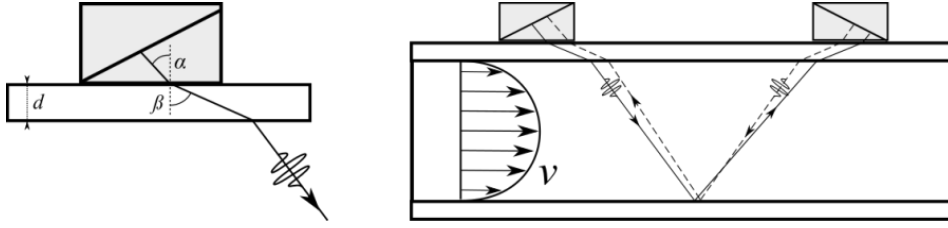


Figure 1: Idealized path of ultrasonic signals in the system of transducer, pipe, and fluid with two passages (reflex mode,  $n=2$ ).

The transit time in the fluid  $t_{Fluid,total}$  depends on the number of passages  $n$  in the fluid. It is calculated from the mean transit time of the two signals  $\bar{t}$  by subtracting the transit time in the pipe wall  $t_{Pipe}$  and the transit time in the transducer wedges  $t_T$ :

$$t_{Fluid,total} = n \cdot t_{Fluid,pass} = \bar{t} - 2t_{Pipe} - 2t_T. \quad (4)$$

According to Snell's law, the length of the sound paths  $s_i$  in a given material is correlated with the speed of sound  $c_i$  of the material. Following these assumptions, Eq. (4) yields:

$$n \cdot t_{Fluid,pass} = \bar{t} - 2 \frac{s_{Pipe}}{c_{Pipe}} - 2t_T = \bar{t} - 2 \frac{d}{c_{Pipe} \cos(\beta)} - 2t_T. \quad (5)$$

The specific parameters of the transducer (acoustic angle  $\alpha$ , speed-of-sound in the transducer  $c_T$ , and transit time in the transducer  $t_T$ ) are stored in the internal database of the processor unit of the measurement device and thus are not accessible for analysis. Therefore, also the acoustic angle in the pipe  $\beta$  cannot be determined. Ultrasonic flow meters use the trigonometric relations to calculate the required distance of the transducer sensors. However, we can use Equation (5) to estimate the influence of pipe material, sensor distance, and number of fluid passages on the overall uncertainty.

The cross-sectional area  $A$  of the pipe is determined by the inner diameter  $D_i$ , which is calculated from the pipe geometry, i.e. wall thickness  $d$  and outer circumference  $L_o$ :

$$A = \frac{\pi}{4} D_i^2 = \frac{\pi}{4} \left( \frac{L_o}{\pi} - 2d \right)^2. \quad (6)$$

As the wall thickness is often measured with ultrasonic methods, the acoustic property of the piping material, i.e. speed-of-sound  $c_{Pipe}$ , and the measured transit time determine the pipe thickness:

$$d = 0.5 \cdot c_{Pipe} t_{Wall}. \quad (7)$$

Typically, the thickness is measured with the same electronics of the flow measurement device but with an additional wall thickness gauge sensor (assumption:  $\alpha = 0$ ).

### 2.3 Heat flow measurement

The heat flow through a heat exchanger  $\dot{Q}$  is calculated from the enthalpy balance with flow and temperature measurements:

$$\dot{Q} = \rho \dot{V} \Delta h(p, T) \approx \dot{V} \rho c_p \Delta T. \quad (8)$$

The fluid properties, i.e. density  $\rho$  and specific heat capacity  $c_p$  are dependent on the temperature of the fluid. However, these properties can be assumed to be constant for small temperature glides  $\Delta T$  for most heat carrier fluids (e.g. water, glycol-water mixtures).

The temperature glide is obtained from measurements with two distinct temperature sensors before and after the heat exchanger.

Combining Equations (3) to (8) we obtain:

$$\dot{Q} = \frac{\pi}{4} \left( \frac{L_o}{\pi} - c_{Pipe} t_{Wall} \right)^2 C_{Profile} C_{Trans} \frac{\Delta t}{2t} \rho c_p \Delta T. \quad (9)$$

### 3. Uncertainty analysis

Equation (9) is used to analyze the uncertainty contributions  $u_{Q,X_i}$  of the different variables  $X_i$  on the final uncertainty of  $\dot{Q}$ .

$$u_{Q,X_i} = \frac{\partial \dot{Q}}{\partial X_i} dX_i. \quad (10)$$

The combined standard uncertainty  $u_{Q,c}$  of  $\dot{Q}$  results from Eq. (11):

$$u_{Q,c} = \sqrt{\sum_i \left( \frac{\partial \dot{Q}}{\partial X_i} u_{Q,X_i} \right)^2} \quad (11)$$

Equation (11) is valid if all specific uncertainties follow a normal distribution, which is assumed for this study. Uncertainties of flow meters as specified by manufacturers typically will not be achieved for field installations. Here we have specified the uncertainties independent from a specific manufacturer or device to elaborate on the most important variables. However, a given calibration certificate of a specific device might also serve as a basis for estimation of uncertainty under best conditions (fully developed flow profile, axial-symmetric flow, etc.).

In the analysis we apply estimated uncertainties which were not obtained from repeated observations what corresponds to a Type B evaluation of the combined uncertainty of the measurement [4].

#### 3.1 Uncertainty of transit time difference and transit time

The measurement of the transit time difference as the basic identifier of the flow magnitude has to be as accurate as possible. Modern processors allow for uncertainties of the transit time difference of less than 50 ps [6].

$$u_{Q,\Delta t} = \frac{\partial \dot{Q}}{\partial \Delta t} d\Delta t = \frac{\pi}{4} \left( \frac{L_o}{\pi} - c_{Pipe} t_{Wall} \right)^2 C_{Profile} C_{Trans} \frac{1}{2t} \rho c_p \Delta T \cdot u_{\Delta t} = \dot{Q} \frac{u_{\Delta t}}{\Delta t} \quad (12)$$

The absolute uncertainty  $u_{\Delta t}$  of the transit time difference measurement is estimated to be 50 ps, independent from laboratory or field conditions. In the analysis the same value is estimated as uncertainty of the transit time  $t$  measured with the transducers and with the wall thickness sensor.

#### 3.2 Uncertainty of flow profile

The modulation of the ultrasonic signal traversing the fluid is influenced by the velocity distribution along the sound path. The correction factor  $C_{Profile}$  compensates for the different methods of averaging, along the path and over the pipe area. It is calculated by the flow meter electronics for an axially symmetric flow. However, the profile may be distorted symmetrically or asymmetrically due to flow disturbances of upstream and downstream installations (pipe bends, reducers, valves, etc.). The effects are dissipated within a straight pipe and are dependent on Reynolds number, distance to the disturbance, circumferential angle of the measuring plane, and inner pipe roughness. A maximum deviation of 3 % was documented for a single-path measurement 4D after a single bend in a flow range of Reynolds 1.5e5 to 2.5e5, with a strong influence of the circumferential position of the measuring plane [7]. A maximum deviation of 25 % 5D after a single bend with single-path measurement is documented in [8]. In general, we consider effects in the order of 5 % as realistic for a single-path measurement in reflex mode after a flow disturbance. To reduce these errors it can be beneficial to measure along two or even more measuring paths. For the example uncertainty calculation we estimate a 0.5 % relative uncertainty for a two-path measurement under laboratory conditions and a 2 % relative uncertainty for a two-path measurement under field conditions.

$$u_{Q, C_{Profile}} = \frac{\partial \dot{Q}}{\partial C_{Profile}} dC_{Profile} = \dot{Q} \frac{u_{C_{Profile}}}{C_{Profile}} \quad (13)$$

### 3.3 Uncertainty of pipe circumference

The circumference of the pipe is used to calculate the cross-sectional area of the pipe. In our study we estimate that simple measuring tape allows for measurements with an uncertainty of  $\pm 1$  mm under field conditions. If special measuring tapes or gauges with Vernier-scale are used, also a lower uncertainty of  $\pm 0.1$  mm can be achieved. This value is used for an estimate under laboratory conditions.

$$u_{Q, L_o} = \frac{\partial \dot{Q}}{\partial L_o} dL_o = \frac{\pi}{4} \left( \frac{2L_o}{\pi^2} - \frac{2c_{Pipe} t_{Wall}}{\pi} \right) C_{Profile} C_{Trans} \frac{\Delta t}{2t} \rho c_p \Delta T \cdot u_{L_o} \quad (14)$$

### 3.4 Uncertainty of pipe material

The speed-of-sound of the pipe material influences the ultrasonic sound path. Most measurement devices include a database with pipe materials to be selected. However, little is known about the variability of the speed-of-sound in a specific material class. In field applications, the exact pipe material might not be known and therefore it has to be estimated. For the analysis, we use a relative standard uncertainty  $u_{c_{Pipe}}$  of 0.1 % under laboratory conditions and of 1.0 % under field conditions.

$$u_{Q, c_{Pipe}} = \frac{\partial \dot{Q}}{\partial c_{Pipe}} dc_{Pipe} = \frac{\pi}{4} \left( \frac{-2L_o t_{Wall}}{\pi} + 2c_{Pipe} t_{Wall}^2 \right) C_{Profile} C_{Trans} \frac{\Delta t}{2t} \rho c_p \Delta T \cdot u_{c_{Pipe}} \quad (15)$$

### 3.5 Uncertainty of thickness of coupling paste

A coupling paste is used to improve the acoustic contact of pipe and wall thickness sensor. We estimate a standard uncertainty of 0.01 mm under laboratory conditions and 0.05 mm under field conditions.

### 3.6 Uncertainty of temperature glide measurement

The accuracy of the temperature measurement is influenced by the accuracy of the calibration procedure, the ambient conditions and the quality of the sensors shielding towards the ambient conditions, the thermal contact to the pipe, and the underlying thermal dynamics of the process. We estimate a standard uncertainty of the temperature glide measurement of 0.03 K under laboratory conditions and 0.1 K under field conditions.

$$u_{Q, \Delta T} = \frac{\partial \dot{Q}}{\partial (\Delta T)} d(\Delta T) = \dot{Q} \frac{u_{\Delta T}}{\Delta T} \quad (16)$$

### 3.7 Uncertainty of fluid properties

The property data of the fluid in the measurement might differ from database values as small amounts of air or gas might be entrained. Additionally, the properties are dependent on temperature and pressure. Whilst the former can be derived from the measurements, the magnitude of pressure is not always available and has to be estimated. For the example calculation we assume a relative uncertainty of 1 % under field conditions. This value might be much higher in case of a heat carrier fluid, such as glycol, with unspecified concentration levels.

$$u_{Q, \rho c_p} = \frac{\partial \dot{Q}}{\partial (\rho c_p)} d(\rho c_p) = \dot{Q} \frac{u_{\rho c_p}}{\rho c_p} \quad (17)$$

### 3.8 Example: Uncertainty of heat flow rate and COP under nominal conditions

As an example, we consider an absorption chiller with nominal capacity of 160 kW (cold water 21-16 °C, cooling water 30-38 °C, hot water 90-72 °C) which was engineered within a research project at TU Berlin (BMW project 0327460) [9]. The cold water circuit and the hot water circuit are designed with DN80 piping connections (outer diameter approximately 88.9 mm, PN16). The nominal capacity of the chiller is provided at

nominal volumetric flow rates of 27.7 m<sup>3</sup>/h at the evaporator and 9.7 m<sup>3</sup>/h at the generator. Its nominal COP is documented with 0.79.

Table 1 lists the uncertainty balance of the variables for a heat flow measurement at the evaporator. Properties of water as a heat carrier fluid were calculated according to IAPWS 1997. The combined uncertainty for this example is 2.0 kW under laboratory conditions and 5.3 kW under field conditions. The generator load with 202.0 kW yields a combined uncertainty of 2.3 kW under laboratory conditions and 5.5 kW under field conditions.

Table 1. Detailed uncertainty calculation for clamp-on measurement at the evaporator of a 160kW chiller under nominal conditions. The transducer parameter is taken from [6] as an example value.

Variable	$x_i$	value	Sensitivity $s_i$		Uncertainty $\Delta x_i$		Uncertainty $s_i \Delta x_i$	
					Lab	Field	Lab	Field
<b>1. Mean velocity</b>	$v$	1.43 m/s	$\partial Q/\partial v$	111.97 kJ/m	0.015	0.033 m/s	<b>1.72</b>	<b>3.69 kW</b>
1.1 Profile parameter	$C_p$	0.95 [-]	$\partial v/\partial C_p$	1.50 m/s	0.005	0.020 [-]	0.008	0.030 m/s
1.2 Beam velocity	$v_B$	1.50 m/s	$\partial v/\partial v_B$	0.95 [-]	0.014	0.014 m/s	0.013	0.013 m/s
1.2.1. Transit time difference	$\Delta t$	48.7 ns	$\partial v_B/\partial \Delta t$	3.1 e7 m/s <sup>2</sup>	50	50 ps	1.54	1.54 mm/s
1.2.2. Transit time fluid	$t_F$	0.14 ms	$\partial v_B/\partial t_F$	-5.4e3 m/s <sup>2</sup>	50	50 ps	-2.70e-4	-2.70e-4 mm/s
1.2.3. Transducer parameter	$C_T$	4300 m/s	$\partial v_B/\partial C_T$	3.5e-4 [-]	40	40 m/s	14.0	14.0 mm/s
<b>2. Cross-sec. pipe area</b>	$A$	5.35e3 mm <sup>2</sup>	$\partial Q/\partial A$	0.03 kW/mm <sup>2</sup>	4.9	44.0 mm <sup>2</sup>	<b>0.15</b>	<b>1.32 kW</b>
2.1 Circumference	$L$	279.3 mm	$\partial A/\partial L$	41.3 mm	0.10	1.00 mm	4.1	41.3 mm <sup>2</sup>
2.2 Pipe thickness	$d$	3.2 mm	$\partial A/\partial d$	-259.2 mm	0.01	0.06 mm	-2.7	-15.3 mm <sup>2</sup>
2.2.1. Speed of sound pipe	$c_{pipe}$	5150 m/s	$\partial d/\partial c_{pipe}$	6.2e-7 s	5	50 m/s	3.1e-3	3.1e-2 mm
2.2.2. Transit time pipe	$t_W$	6.21e-7 s	$\partial d/\partial t_W$	5150 m/s	50	50 ps	2.6e-4	2.6e-4 mm
2.2.3. Coupling paste thickness	$d_c$	0.05 mm	$\partial d/\partial d_c$	1 [-]	0.01	0.05 mm	0.01	0.05 mm
<b>3. Temperature glide</b>	$\Delta T$	5.0 K	$\partial Q/\partial \Delta T$	31.9 kW/K	0.03	0.1 K	<b>0.96</b>	<b>3.19 kW</b>
<b>4. Fluid properties</b>	$\rho c_p$	4179 MJ/m <sup>3</sup> K	$\partial Q/\partial \rho c_p$	0.04 m <sup>3</sup> /ksK	4.18	41.8 MJ/m <sup>3</sup> K	<b>0.16</b>	<b>1.60 kW</b>
<b>Combined uncertainty (Eq. 11)</b>							<b>2.0</b>	<b>5,3 kW</b>

With these results, the combined standard uncertainty of non-invasive metering of the COP is 0.01 under laboratory conditions and 0.03 under field conditions. Thus, the extended standard uncertainty (k=2) of the COP yields 0.03 under laboratory and 0.07 under field conditions (Table 2).

Table 2. Standard uncertainties of the main heat flows and of the COP under nominal conditions.

Value	nominal	Laboratory		Field	
	Value	abs.	rel.	abs.	rel.
$\dot{Q}_0$ (kW)	160	2,0	1,2%	5,3	3,3%
$\dot{Q}_2$ (kW)	202	2,2	1,1%	5,5	2,7%
$COP$	0,79	0,01		0,03	
$u_{C,COP}$ (k=2)		<b>0,03</b>	<b>3,4%</b>	<b>0,07</b>	<b>8,6%</b>

### 3.9 Uncertainty with varying flow rates

Evidently, the overall uncertainty is highly dependent on the volumetric flow rate and on the temperature glide at the main heat exchangers. For a constant nominal capacity of 160 kW at the evaporator the effect of flow rate variation on the measurement variance is documented in Figure 2. For simplicity, this calculation does not include the feedback of a flow rate variation on the heat transfer in the evaporator. Variance is depicted instead of uncertainty to allow for a better differentiation of the influences of the uncertainties of cross-sectional area, fluid properties, temperature glide, and flow velocity.

At a nominal flow rate of 27.7 m<sup>3</sup>/h, the measurement uncertainty is dominated by the uncertainties of the temperature and flow measurement. Reducing the flow rate the variance of the temperature glide tends to zero while the variance of velocity passes a minimum. An overall minimum variance of 17.8 (kW)<sup>2</sup> is achieved at this capacity at a flow rate of 6.2 m<sup>3</sup>/h and a temperature glide of 22 K. Note that this flow variation cannot necessarily be applied onto the field application as its range might be limited by the hydraulic system.

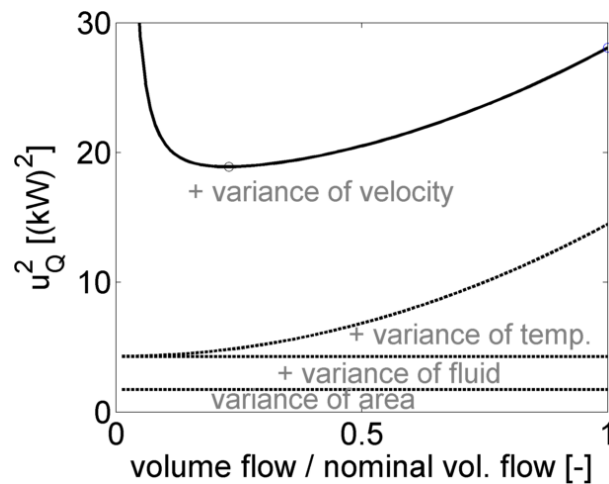


Fig. 2. Dependence of variance with respect to the normalized volumetric flow rate of an evaporator with 160 kW heat capacity under field conditions. The nominal volumetric flow rate is 27.7 m<sup>3</sup>/h.

### 3.10 Uncertainty under part-load conditions

Most heat-pumps operate in part load most of the operational time and monitoring can reveal optimization potential especially under these conditions. The ESEER is a performance indicator of the part load efficiency of an electrical chiller. According to [5] it can also be adapted to thermally driven heat pumps. The analyzed operating points are at 25%, 50%, 75% and 100% of the full load capacity. The standard does not define how the part load may be controlled, either with constant flow rates, or with varied flow rates and adapted temperatures, or with a combination of these modes. To obtain an estimate of the maximum uncertainties under part load conditions, this study assumes constant efficiency and two modes of operation: (1) variation of temperature glide at constant flow rates at the heat exchangers; (2) variation of flow rate at constant temperature glide at the heat exchangers.

As can be seen in Table 3, the relative standard uncertainty of the EER increases with decrease of the loads at the chiller. Operating with constant volumetric flow rates yields the highest uncertainties under both laboratory and field conditions. At 25% part-load, the relative standard uncertainty amounts to 9.1% at a constant flow rate whilst it is at 4.4% for a constant temperature glide. Applying a typical set of weighting coefficients (0.03 at 100% load, 0.33 at 75% load, 0.41 at 50% load, and 0.23 at 25% load) the relative standard uncertainty of the ESEER amounts to 2.1% for constant flow rate and 1.8% for constant temperature glide under laboratory conditions. It amounts to 6.1% and 4.3% under field conditions, respectively.

Table 3. Standard uncertainties of the main heat flows and of the COP in part-load for two modes of operation (1) variation of temperature glides at constant flow rates at the heat exchangers ( $\dot{V}=\text{const}$ ); (2) variation of flow rates at constant temperature glides at the heat exchangers ( $\Delta T=\text{const}$ ) und laboratory and field conditions.

Value		Laboratory		Laboratory		Field		Field	
		$\dot{V}=\text{const}$		$\Delta T=\text{const}$		$\dot{V}=\text{const}$		$\Delta T=\text{const}$	
		abs.	rel.	abs.	rel.	abs.	rel.	abs.	rel.
$\dot{Q}_0$	160 kW	1,98	1,24%	1,98	1,24%	5,30	3,31%	5,30	3,31%
	75% 120 kW	1,61	1,34%	1,49	1,24%	4,50	3,75%	3,98	3,32%
	50% 80 kW	1,29	1,61%	1,00	1,25%	3,83	4,79%	2,65	3,31%
	25% 40 kW	1,05	2,63%	0,52	1,30%	3,36	8,40%	1,33	3,33%
$\dot{Q}_2$	202 kW	2,29	1,13%	2,29	1,13%	5,50	2,72%	5,50	2,72%
	75% 152 kW	1,73	1,14%	1,76	1,16%	4,19	2,76%	4,14	2,73%
	50% 101 kW	1,18	1,17%	1,25	1,23%	2,92	2,88%	2,80	2,77%
	25% 51 kW	0,66	1,30%	0,81	1,60%	1,75	3,46%	1,49	2,94%
COP	0,79	0,01	1,68%	0,01	1,68%	0,03	4,28%	0,03	4,28%
	75% 0,79	0,01	1,76%	0,01	1,70%	0,04	4,66%	0,03	4,29%
	50% 0,79	0,02	1,99%	0,01	1,76%	0,04	5,59%	0,03	4,31%
	25% 0,79	0,02	2,93%	0,02	2,06%	0,07	9,08%	0,04	4,44%

#### 4. Discussion

The analysis has shown that the uncertainty of non-invasive measurements strongly depends on flow rate and temperature glide. For any heat exchanger with a set capacity one configuration of temperature glide and volumetric flow rate with a minimum measurement uncertainty exists. Consequently, also the COP of a heat pump has a minimum uncertainty for one specific combination of the flow rates at the heat exchangers. These flow rates are in most cases not in accordance to the nominal flow rates. Further effects, such as fluid properties and the pipe geometry are also of importance, especially under field conditions. Therefore, the measurement procedure has to be optimized for each specific installation.

The results of the example calculation have shown that the nominal COP can be measured with an extended uncertainty ( $k=2$ ) as precise as 0.03 under laboratory conditions and as precise as 0.07 under field conditions. While the former value can be considered to be acceptable for heat-pump analysis, it is obvious that with the latter value only significant deviations from the expected operational behavior can be detected. It is therefore necessary to use the best methods possible to reduce the influences of temperature glide measurement and flow profile analysis. Particularly, if part-load operation is analyzed and seasonal performance indices are applied it is of utmost importance to minimize uncertainties by a guided measurement. The results of the example calculation have shown that the relative extended standard uncertainty ( $k=2$ ) of the part load performance increases up to 0.14 (18.2%) for an operation with constant volumetric flow rate at a part load of 25%. The large uncertainty can be attributed primarily to the lower accuracy of the temperature glide measurement. Under such conditions the measurements should be improved by flow rate variation. For constant temperature glide the uncertainty was halved.

High measurement accuracy is required, if the measurements are used to compare with the specifications or a previous measurement after re-installation. Under such circumstances the non-intrusive technique might not be applicable. For direct fired sorption heat pumps it is of utmost importance to measure the internal enthalpy of the gas flow which is dependent on pressure. With this non-invasive technology only measurements at the intermediate circuit and at the evaporator circuit are possible and the method cannot be used to characterize gas fired heat pumps without further inline metering.

The documented uncertainties have a systematic influence on the measurement. Effects that have a lower magnitude than the above documented uncertainties can be differentiated if the measurement equipment is used as fixed installation. Thereby the method can be applied to quantify also smaller changes in the operational behavior, such as the effect of adapted flow rates, evacuation of non-condensable gases, or the impact of an addition of surfactants.

For most of the applied uncertainties quantified measurements are missing and they could only be estimated. Furthermore, there exists a knowledge gap on how measurement results are influenced by the installation process, e.g. by deviations of the path from the axial plane, or differences in coupling paste consistency. The study has neglected dynamic effects which might result in a further increase of the uncertainties. Further studies should examine and quantify these effects.



## 5. Conclusion

As efficiency of energy systems becomes more important, non-intrusive methods for characterizing installed heat pumps will attract more attention. Measurements of heat flows have to be accurate and should be based on a pre-analysis of the combined uncertainty. The study analyzed the measurement uncertainties of the COP of an example chiller in nominal and part-load operation. Although measurements under laboratory conditions can be as precise as 0.03 (expanded uncertainty with  $k=2$ ), the accuracy is significantly lower under field conditions and in part-load operation.

Characterization of heat pumps can be optimized by variation of the volumetric flow rate. Especially in the case of a large contribution of the temperature glide measurements to the combined uncertainty, it is useful to reduce the volumetric flow rate. Measurements under field conditions might benefit from an expert system that optimizes the measurement configuration with a software-assisted uncertainty assessment. Furthermore, corrections of the systematic effects, such as the influence of flow disturbances, with a physical modelling can increase the measurement accuracy.

## Acknowledgements

This study is funded by Bundesministerium für Wirtschaft und Energie (Federal Ministry for Economic Affairs and Energy) with research grant 01164633/1 (“EnEff:Wärme - nivEx: Optimierung eines mobilen nicht-invasiven Messverfahrens zur Verbesserung der Energieeffizienz von Wärmeübertragungssystemen”).

## References

- [1] Kühn, A.; Graf, R; Corrales Ciganda, J.; Schmitt-Gehrke, P.; Gassenmeyer, F.; Blum, N. (2016), “Betriebsstrategien für Gasabsorptionswärmepumpen“, technical report, project: 1320UEPII/2, <https://www.eta.tu-berlin.de/.../projekte/>
- [2] M. Miara, D. Günther, T. Kramer, T. Oltersdorf and J. Wapler, Heat Pump Efficiency: Analysis and Evaluation of Heat Pump Efficiency in Real-life Conditions, Fraunhofer ISE, 2011
- [3] Miara, M., Günther, D., Kramer, T., Oltersdorf, T. und Jeannette Wapler (2011). “WP Monitor: Feldmessung von Wärmepumpenanlagen.” URL: [https://wp-monitor.ise.fraunhofer.de/german/index/das\\_projekt.html](https://wp-monitor.ise.fraunhofer.de/german/index/das_projekt.html)
- [4] Bureau International des Poids et Mesures, Commission électrotechnique internationale, and Organisation internationale de normalisation (1995). Guide to the Expression of Uncertainty in Measurement. International Organization for Standardization.
- [5] IEA Heat Pump Centre (2016). Annex 34: Thermally Driven Heat Pumps for Heating and Cooling, final report, ISBN 978-91-87461-60-6.
- [6] Funck, B. (2016). “US-Clamp-On-Zähler: Schritte in Richtung auf die Rückführbarkeit“ 12. Internationale EMATEM-Sommerschule, 21. - 23. Sep. 2016, Seeon, Germany.
- [7] Merzkirch, W. et al. (2005). Fluid mechanics of flow metering. Heidelberg, Germany: Springer, 2005.
- [8] Patent application DE102013106108 (A1) (2014): Method for ascertaining a compensated flow and/or a compensated flow speed, ultrasonic flow measuring device, and computer program product. Published 31. Dec. 2014.
- [9] Meyer, F. (2012). Mit Wärme kühlen. BINE Projektinfo 07/2012. [http://www.bine.info/fileadmin/content/Publikationen/Projekt-Infos/2012/Projekt\\_07-2012/ProjektInfo\\_0712\\_internetx.pdf](http://www.bine.info/fileadmin/content/Publikationen/Projekt-Infos/2012/Projekt_07-2012/ProjektInfo_0712_internetx.pdf).